SIMULATING ACID MINE DRAINAGE THROUGH MINE WASTES CONSTRUCTED WITH CAPILLARY BARRIER COVERS

J.W. Molson[1], M. Aubertin[1,*], B. Bussière[2,*] & A-M. Joanes[3]
(1) Dept. of Civil, Geological and Mining Engineering, Ecole Polytechnique, Montreal
(2) Université du Québec en Abitibi-Témiscamingue, Rouyn-Noranda
*NSERC-Polytechnique-UQAT Chair, Environment and Mine Waste Management
(3) Now with the Ministère des Ressources Naturelles, de la Faune et des Parcs du Québec

ABSTRACT
The evolution of acid mine drainage (AMD) from reactive mine wastes is simulated using the MIN3P finite volume model for coupled groundwater flow, oxygen diffusion and multi-component reactive transport including sulphide oxidation and mineral precipitation and dissolution. The model is applied to a field test cell experiment designed with a capillary barrier effect cover (CCBE) over reactive tailings from the Manitou mine, Val d'Or, Quebec. The preliminary simulations support the conclusion that sulphide oxidation and acid mine drainage can be significantly reduced using capillary barriers. The simulations of the in-situ cell without a CCBE cover reflected extensive sulphide oxidation, including low-pH and elevated concentrations of iron and sulphate. When the same tailings were simulated with a CCBE cover, the predicted drainage was relatively pH-neutral. The results were consistent with the observed data. The model is providing important new insights for comparing design alternatives for reducing or controlling AMD.

RÉSUMÉ
Le développement du drainage minier acide (DMA) généré par des rejets miniers réactifs est simulé par l'utilisation du modèle MIN3P, considérant le débit des eaux souterraines, la diffusion de l'oxygène et le transport des composants réactifs, y compris l'oxydation des sulfures, la précipitation et la dissolution de minéraux. Le modèle numérique est appliqué à une cellule expérimentale in situ constituée de rejets réactifs recouverts d'une couverture avec effets de barrière capillaire construite sur le site de la mine Manitou à Val-d'Or au Québec. Les simulations ont montré que l'oxydation des sulfures et le drainage minier acide peuvent être considérablement réduits par l'utilisation de barrières capillaires. Les résultats observés et ceux simulés pour une cellule in situ non recouverte montrent une oxydation à grande échelle des sulfures, incluant un bas pH et des concentrations élevées de fer et de sulfates. Une simulation sur une cellule identique, avec une couverture à effets de barrière capillaire, montre un drainage avec peu d'oxydation des sulfures. Ce nouvel outil de simulation apporte de nouvelles méthodes prometteuses pour la réduction et le contrôle du DMA.

1. INTRODUCTION

Waste rock piles and mill tailings which contain sulphide minerals can be significant sources of acid mine drainage (AMD). Oxidation of pyrite or pyrrhotite, for example, will often produce AMD characterized by a low-pH, and high concentrations of sulphate, iron and other dissolved metals which are potentially toxic to the environment (Jambor, 1994; Sracek et al., 2003). Research is advancing on characterizing these types of mine wastes, understanding the reactive processes responsible for AMD as well as developing new methods of prevention and remediation (Blowes et al., 1994; Lefebvre et al., 2001; Schneider et al., 2002).

The rate of AMD generation from porous mine wastes depends to a large degree on the diffusive flux of oxygen, which decreases as the water content increases (e.g. Aachib et al., 2002). Several strategies for reducing AMD are therefore based on increasing the water content of mine wastes. Two of the more common approaches involve waste flooding (applicable primarily to tailings in low-lying areas), and the use of various cover materials including covers with capillary barrier effects (CCBEs).

The behaviour of CCBEs is based on the contrast in water retention characteristics between fine and coarse grained porous materials. Typically, in a wet climate setting, a fine-grained layer is sandwiched between two coarser grained layers. If placed under negative pressure (in unsaturated conditions), the coarse layers will drain rapidly to a residual water content while the fine layer will remain close to saturation (Nicholson et al., 1989; Aubertin et al. 1999; Bussière et al., 2003).

Emplaced at the surface of AMD-generating tailings, a cover with a capillary barrier effect can reduce the rate of oxygen diffusion, thereby reducing the rate of sulphide oxidation. Capillary barriers have also been proposed to reduce oxygen diffusion through waste rock piles, and can be used to control internal fluid flow (Bussière et al., 2003; Mbonimpa et al., 2003; Molson et al., 2004).

Numerical simulation models are useful tools for predicting the behaviour of CCBEs (e.g. Bussière, 1999, Oldenburg & Pruess, 1993), and for predicting flow and reactive transport through mine wastes. Lefebvre et al. (2001), for example, used the TOUGH/AMD model (Pruess, 1991) to simulate flow, oxygen transport and pyrite oxidation within a waste rock pile. Romano et al. (2003) applied the PYROX model (Wunderly et al., 1996) to simulate AMD from 1D waste columns constructed with various cover scenarios. In each of these approaches, only the immediate oxidation products (H+, Fe^{2+} and SO_4^{2-}) were simulated; the full geochemical system including geochemical speciation and pH buffering by solid minerals was not considered. Mayer et al. (2003) provide an overview of the latest developments in reactive transport models for mine waste applications.

In this paper, the numerical model MIN3P (Mayer et al., 2002) is used to help gain insight into the application of capillary barrier covers for reducing AMD. The model is applied to simulate an experimental in-situ test cell in which a CCBE cover was emplaced over reactive tailings from the Manitou mine site, Val d'Or, Quebec (Bussière, 1999; Bussière and Aubertin, 1999; Aubertin et al., 1999; Bussière et al., 2001). The results are compared to an equivalent waste cell covered only with sand.

2. FIELD EXPERIMENT SET-UP

The field site included six pilot-scale emplaced cells, in the shape of inverted pyramids each measuring about 11x11m at the surface and 3m deep at the centre (Figure 1). Each cell was underlain by an impervious geomembrane which channelled drainage water to a subdrain. The top surface of each cell was open to natural infiltration and the drainage water was monitored for AMD over a 4-year period.

The base of each test cell was filled with 1.5m of sulphidic waste from the Manitou mine. In cells 1-5, the tailings were overlain by 0.4m of non-reactive sand, followed by a fine grained moisture-retaining layer (as the capillary barrier), then covered at surface by a final 0.3m layer of sand. The moisture retaining layer was different for each cell and was composed of various combinations of non-reactive fine mine residue (from the Sigma mine, Quebec) or natural till. Cell 6 included only the 1.5m of reactive tailings, with no capillary barrier cover. In this study, we will focus on the CCBE covered Cell 1 and the non-CCBE covered Cell 6.

Laboratory column experiments with the same reactive mine waste and covers were also run prior to and concurrent with the field trials (Joanes, 1999; Aubertin et al., 1999). The complete laboratory experiment included a series of 5 plexiglass columns with heights ranging from about 1.5 to 2.0m depending on the cover scenario. The results were consistent with those obtained from the field therefore in this paper, we will focus primarily on the field experiment.

3. NUMERICAL MODEL

3.1 Flow Equation

The MIN3P model solves the governing equation for Darcy-type fluid flow in a variably-saturated porous medium. Assuming a passive air phase, the mass conservation equation for the water phase can be written as:

$$S_a S_s \frac{\partial h}{\partial t} + \theta \frac{\partial S_a}{\partial t} - \nabla \times \left[k_{ra} \overline{K} \nabla h \right] - Q_a = 0 \qquad [1]$$

where S_a is the aqueous phase (water) saturation (L^3L^{-3}), S_s is the specific storage coefficient [L^{-1}], h is the hydraulic head [L], t is time [T], θ is the porosity [L^3L^{-3}], Q_a is a source-sink term [T^{-1}], k_{ra} is the relative permeability of the porous medium with respect to the water phase [-] and $\overline{K}$ is the saturated hydraulic conductivity tensor [LT^{-1}].

The non-linear functions defining water saturation and relative permeability are given by van Genuchten (1980) and Wösten and van Genuchten (1988), according to:

$$S_a = \frac{\theta_w - \theta_r}{\theta - \theta_r} = \left[\frac{1}{1 + (\alpha_v \psi)^n} \right]^m \qquad [2]$$

$$k_{ra} = S_a^{\ell} \left[1 - \left(1 - S_a^{1/m} \right)^m \right]^2 \qquad [3]$$

where θ_w is the water content, θ_r is the residual water content, ψ is the water pressure, α_v, n and m are the van Genuchten parameters determined from the moisture retention curve (with m=1-1/n), and ℓ is a parameter representing the degree of pore connectivity (ℓ=0.5 is used here).

3.2 Transport Equation

The transport equation for advective-dispersive transport of multiple, dissolved phase components, including diffusive gas transport and reactive source-sink terms (from mineral precipitation & dissolution, phase exchange etc.), is written as:

$$\frac{\partial}{\partial t}\left[S_a\theta\cdot T_j^a\right]+\frac{\partial}{\partial t}\left[S_g\theta\cdot T_j^g\right] + \nabla\times\left[q_a T_j^a\right]-\nabla\times\left[S_a\theta\cdot D_a\nabla T_j^a\right] - \nabla\times\left[S_g\theta\cdot D_g\nabla T_j^g\right] - Q_j^{a,a}-Q_j^{a,s}-Q_j^{a,ext}-Q_j^{g,ext}=0 \quad [4]$$

where S_g is the gas phase saturation, T_j^a and T_j^g [ML^{-3}] are the total aqueous and gas phase concentrations of component j, respectively, q_a [LT^{-1}] is the Darcy flux and D_a and D_g [L^2T^{-1}] are the dispersion tensors for the aqueous and gas phase components, respectively. The source-sink terms $Q_j^{a,a}$ and $Q_j^{a,s}$ represent contributions to T_j^a from intra-aqueous and precipitation-dissolution reactions, respectively. Similarly, $Q_j^{a,ext}$ and $Q_j^{g,ext}$ represent external source-sinks for the aqueous and gas phases, respectively.

Transport of oxygen through a partially saturated porous medium is governed by the effective diffusion coefficient D_e [L^2T^{-1}] which in MIN3P is based on the Millington-Quirk (1961) model written as:

$$D_e = D_g^o\frac{S_g^{10/3}}{\theta^{4/3}}+HD_a^o\frac{S_a^{10/3}}{\theta^{4/3}} \quad [5]$$

where D_g^o and D_a^o are the diffusion coefficients [L^2T^{-1}] of oxygen in the gas and aqueous (water) phases, respectively, and H is Henry's Law constant ($[O_{2w}]/[O_{2a}]$ at equilibrium). Equation 5 is equally valid for partially saturated, or water or gas-saturated conditions. In this study, we will use the optional shrinking core model within MIN3P, which simulates diffusion-controlled pyrite oxidation assuming a spherical grain geometry (Davis and Ritchie, 1986).

MIN3P uses a control volume, global implicit solution method which is locally mass conservative. Newton iteration is employed to linearize both the flow and transport equations. Upstream weighting, and adaptive time stepping were chosen for this study. Further details on the numerical solution approach and handling of ion-exchange and mineral precipitation-dissolution reactions are given in Mayer et al. (2002).

4. GEOCHEMICAL SYSTEM AND MATERIAL PROPERTIES

The test cell shown in Figure 1 (corresponding to field Cell 1) is here considered as a vertical 1D column 2.8 m long. The column is discretized uniformly using 101 control volumes.

Two cover scenarios will be considered: Case 1 is a column of reactive mine waste covered only with a layer of clean sand, while Case 2 is an identical column covered with a capillary barrier effect cover (Figure 2). Each case includes 1.5m of sulphide-containing waste at the base. Case 1 corresponds to the Manitou Field Control Cell 6, while Case 2 corresponds to Field Cell 1.

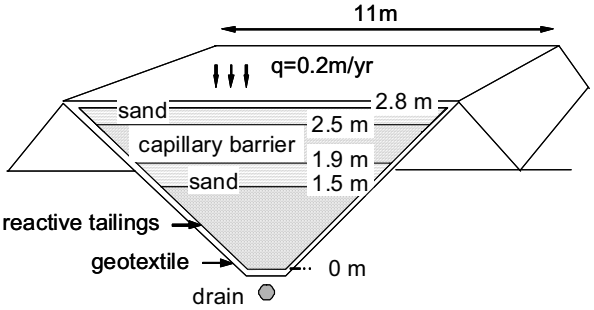

Figure 1. Conceptual model of the CCBE-covered in-situ test cell #1 (Case 2 in this study).

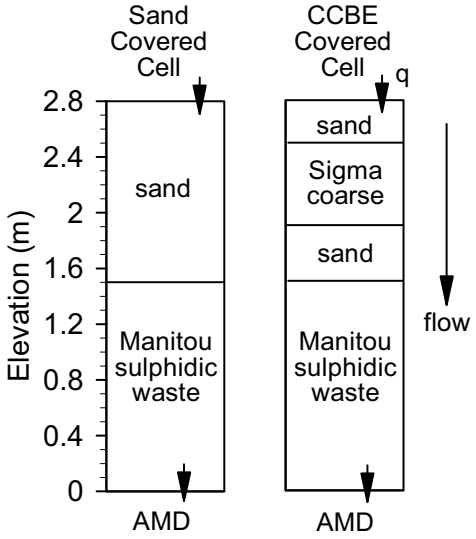

Figure 2. Structure of the sand- and CCBE-covered cells as incorporated in the 1D numerical model (Case 1 and 2, respectively).

Note that as installed in the field, Cell 6 (Case 1 here) included only the 1.5m of waste, without a cover. A 1.3m sand cover was added to the Case 1 model to facilitate comparison with the CCBE-covered model cell (Case 2). Fully uncovered simulations (not shown) confirmed that since the flow system reached steady state relatively quickly, and the sand was sulphide-free, the added sand column in Case 1 had no effect on the AMD predictions.

Three porous materials are considered in the two models: the reactive Manitou mine wastes, the fine-grained capillary barrier made of sulphide-free waste from the

Sigma Mine, and a sulphide-free sand. Material properties affecting the moisture-retention behaviour for each layer are provided in Table 1 and the water retention and hydraulic conductivity curves are provided in Figure 3.

In both columns, we consider 13 aqueous components, 2 redox pairs, 25 secondary species, 2 gases and 10 minerals (Table 2). Reaction stoichiometry and mineral formulae can be found in Mayer et al. (2002).

Table 1. Material Properties for the in-situ test cell experiments (after Aubertin et al., 1999). The "Sigma Coarse" material was used as the capillary barrier, while the Manitou unit formed the reactive tailings.

Material	θ	θ_r	K_{zz} [m/s]	α_v, n [1] [m^{-1}], [-]	AEP [m]
Sand	0.40	0.03	7.2×10^{-5}	2.9, 10.2	0.28
Sigma Coarse	0.41	0.08	1.5×10^{-6}	0.15, 2.6	2.75
Manitou	0.42	0.07	2.7×10^{-5}	0.61, 2.6	2.65

[1] van Genuchten parameters (λ=0.5 for all materials)
AEP = Air Entry Pressure

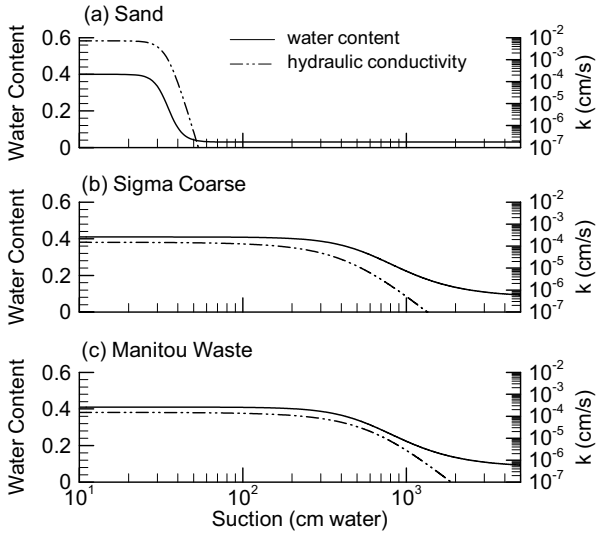

Figure 3. Water retention and hydraulic conductivity curves for each of the cell materials used in the model. Curves are defined by equations (2) and (3), using parameters from Table 1.

Mineralogical analyses of the Manitou sulphide-bearing waste by X-ray diffraction showed an abundance of quartz (60%), followed by sericite (15%), chlorite (9%), pyrite (5.5%), feldspars (5%) and gypsum (3%) (Aubertin et al., 1999, Annex). Traces of carbonates were also found. Mineralogical data for the Sigma Coarse capillary barrier was less precise, but was also dominated by quartz and feldspars with some chlorite and biotite. Carbonate content, including calcite and ankerite, was also higher for the Sigma Coarse layer, estimated at up to 10%.

In the numerical model, the primary sulphide mineral in the Manitou mine waste is assumed to be pyrite, with the overall oxidation reaction stoichiometry given by:

$$FeS_{2(s)} + 7/2\ O_2 + H_2O \rightarrow Fe^{2+} + 2SO_4^{2-} + 2H^+ \qquad [6]$$

Pyrite is assumed to be uniformly distributed within the Manitou tailings at an initial volume fraction of 0.05 (5%). The initial unoxidized grain diameter is taken to be 0.1mm, corresponding with the most abundant fraction (Aubertin et al., 1999, Annex).

Table 2. Summary of all components considered in the geochemical transport model.

Aqueous Components: Ca^{+2}, K^{+1}, Cl^{-1}, H_4SiO_4, Al^{+3}, CO_3^{-2}, H^{+1}, O_2(aq), Fe^{+2}, SO_4^{-2}, Fe^{+3}, HS^{-1}, Mg^{+2}
Redox Couples: Fe^{+2} / Fe^{+3} SO_4^{-2} / HS^{-1}
Secondary Aqueous Species: OH^-, $H_3SiO_4^-$, $CaHCO_3^+$, $CaCO_{3aq}$, $CaSO_{4aq}$, KSO_4^- $Al(OH)_2^+$, $Al(OH)_4^-$, $Al(OH)_{3aq}$, $FeOH^+$, $FeSO_{4aq}$ HCO_3^-, H_2CO_{3aq}, $AlOH^{+2}$, $AlSO_4^+$, $Al(SO_4)_2^-$ HSO_4^-, $FeOH^{+2}$, $FeSO_4^+$, $FeOH^{2+}$, $Fe(OH)_{3aq}$ $MgSO_{4aq}$, $MgCO_{3aq}$, $MgOH^+$, $MgHCO_3^+$
Gases: O_2(g) , CO_2(g)
Solid Minerals (with initial volume fractions): pyrite (waste f_v =0.05; all cover materials f_v =0.00) calcite (0.0001) — jarosite (0.00) siderite (0.002) — k-feldspar (0.05) gibbsite (0.005) — biotite (0.05) gypsum (0.02) — quartz (a,pt) (0.6) ferrihydrite (0.00) — + non-reactive minerals

To simplify the conceptual model, and to focus on the effect of the capillary barrier, it was assumed, with the exception of the sulphide content, that the Manitou waste, Sigma Coarse and sand layers had identical mineralogy as shown in Table 2. Only the most reactive of the observed mineral phases were included, and where the observed mineral fractions differed, an average was used. In each cell, pyrite was assumed to exist only in the Manitou waste layers. Jarosite and ferrihydrite were assumed initially not present but were allowed to precipitate as secondary minerals. The mineralogy in Table 2 also reflects the adjustments made during the

calibration of the model to the observed pH and SO_4 concentrations.

The 1D model columns are open at the top and bottom, and the sides are impermeable. A steady recharge of 0.36 m/yr is applied at the top inflow boundary, and is assigned a typical chemical composition of rainwater which has been equilibrated with atmospheric oxygen (for assumed rainwater composition, see Mayer et al., 2002).

At the top surface, oxygen is fixed at its atmospheric concentration (0.2 mg/L_{air}). The water pressure is fixed at the base at 0.0 m, allowing free drainage. The columns are assumed initially water saturated and oxygen-free. Effects of temperature, including winter freezing, are not considered.

The dispersivity for each material is assumed 0.5 mm, and the free diffusion coefficients in water (2.38×10^{-9} m^2/s), and in air (2.07×10^{-5} m^2/s) are assumed constant for all components.

5. EXPERIMENTAL & NUMERICAL RESULTS

The models were run for a 1200 day period, beginning after cell emplacement on September 1, 1995. Execution times were typically on the order of 15-20 minutes on a Pentium IV, 2GHz machine.

Results are provided in Figures 4 and 5 for Case 1 (sand cover) and Case 2 (CCBE cover), respectively. In each figure, the transient response is shown for pressure, saturation, oxygen, pH and pyrite volume fraction (f_v), while only the 1200-day solution is shown for the selected solid minerals and aqueous components.

5.1 Case 1: Sand-Covered Cell

In Case 1 (Figure 4), the reactive wastes are covered only with clean sand, there is no capillary barrier cover. The vertical water pressure and saturation profiles show that water is rapidly drained from the sand, leaving a steady state saturation after 10 days of about 0.1. In comparison, the saturation within the finer-grained and less permeable reactive wastes remains somewhat higher, at about 0.4-0.5.

As the sand cover drains and the water content decreases, oxygen diffuses rapidly inwards from the top surface boundary, advancing about 1m after 2 days. When the oxygen front reaches the upper boundary of the reactive wastes at 1.5m elevation, oxygen begins to be rapidly consumed due to pyrite oxidation. The rate of advance of the diffusion front therefore decreases and the diffusion profile becomes bilinear. After 1200 days, the oxygen front has advanced about 1.6m into the column.

As the pyrite is oxidized, a low-pH zone develops with the trailing (upgradient) edge corresponding to the oxygen diffusion front (Figure 4). This low-pH water is carried downwards with the natural infiltration, and the low-pH zone gradually widens. A corresponding pyrite-"dissolution" front develops when the pyrite becomes completely oxidized. The pyrite oxidation front in this case advances about 0.3m in 1200 days.

The low-pH zone shows three distinct plateaus which can be correlated with a sequence of solid buffering minerals. Calcite, for example, buffers the pH at about 6.5-7. As calcite dissolves, siderite temporarily forms the next pH buffer at about pH~5. The siderite plateau is limited in duration because siderite rapidly dissolves as the pH declines further. Gibbsite then buffers the pH at about 4, while ferrihydroxide and the various silicate minerals help buffer the pH at lower levels. Similar patterns of sequential mineral buffering have been observed and simulated by Bain et al. (2003), Jurjovec et al. (2002), and Johnson et al. (2000).

In this sand-covered cell, the minimum simulated pH within the column dropped to about 1 which is somewhat lower than the observed minimum in the discharge water (pH~2-3). The difference may be due to an incomplete background mineralogy assumed in the model.

The mineral volume fraction profile shows that after 1200 days, calcite and gibbsite remain at their initial fractions within the sand cover, while some ferrihydrite has precipitated. Within the low pH zone of the mine tailings, calcite, siderite, gibbsite and ferrihydrite are completely dissolved, and jarosite has precipitated in the pyrite-depleted zone due to higher SO_4 levels from pyrite oxidation. Gypsum, feldspar and silica (not shown) remain relatively unchanged.

The oxidation of pyrite also releases dissolved iron and sulphate which react with other species and are transported downward through the column pore water. In this case, total iron (predominantly Fe^{2+}) and sulphate concentrations reach about 0.5 and 1 mol/L, or $0.3x10^5$ and $1x10^5$ ppm, respectively, which are consistent with levels observed in the uncovered field cell (Cell 6, Aubertin et al, 1999; Bussière and Aubertin, 1999). The acidic pore waters also dissolve gibbsite which releases Al^{+3}. In this case, simulated Al^{+3} concentrations reached 0.01 mol/L, or 270 ppm.

5.2 Case 2: CCBE-Covered Cell

In Case 2 with the capillary barrier cover (Figure 5), the transient response over the first 60 days shows that the water again drains rapidly from the sand, however the capillary barrier between 1.9 and 2.5m elevation remains close to saturation (S_a>0.9). The steady state saturation within the reactive Manitou mine waste (~0.4-0.5) is still above that of the two sand layers (0.1), but remains significantly less than the saturation of the capillary barrier. These results are consistent with those obtained by Bussière (1999) and Joanes (1999) using the SEEP model.

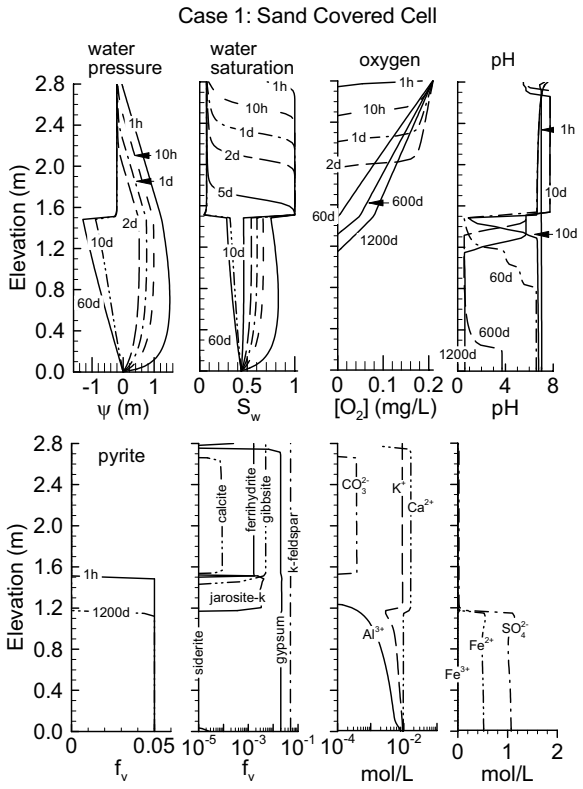

Figure 4. MIN3P numerical simulation showing vertical profiles for Case 1: sand-covered Manitou mine waste without a capillary barrier.

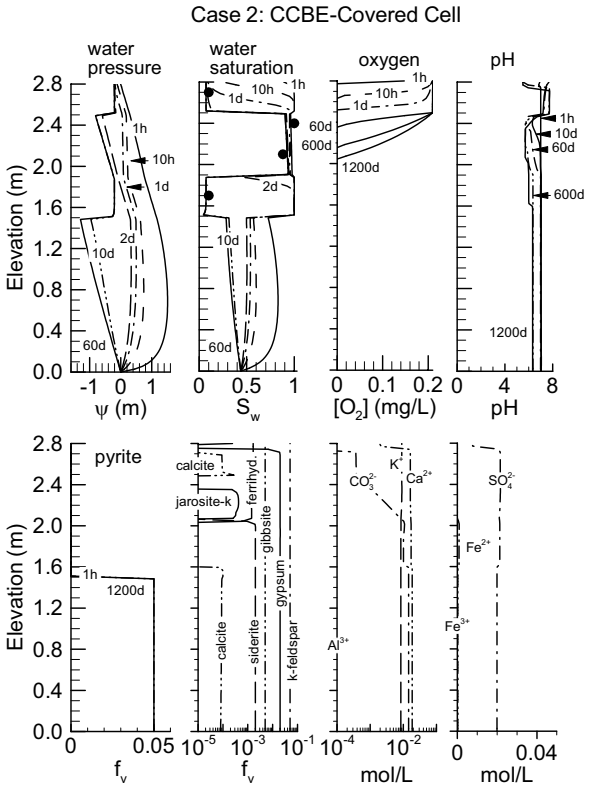

Figure 5. MIN3P simulation showing vertical profiles for Case 2: Manitou mine waste with a capillary barrier effect cover. Observed data (Aubertin et al., 1999; p159) are superimposed on the saturation profile.

Within 2 days of the start of drainage in Case 2, the oxygen front has advanced about 0.3 m into the column from the top surface, but as the front enters the nearly-saturated capillary barrier, the diffusive flux is significantly reduced. After 1200 days, for example, the front has only advanced 0.8 m from the top surface.

The higher water saturation in the capillary barrier has thus significantly reduced the flux of oxygen into the column. In this case with the capillary barrier cover, the pH remains neutral, there is no pyrite-oxidation front, and concentrations of Fe^{2+} and SO_4^{2-} are about 2 orders of magnitude less than in the non-CCBE cover scenario. Also, since the pH is neutral, gibbsite does not dissolve and Al^{+3} concentrations remain very low (<0.01 ppm).

Because of the neutral pH within the CCBE-covered mine tailings, siderite has not been completely dissolved even after 1200 days. Jarosite, which precipitated in the lowest pH region of the sand-covered waste (Figure 4), is here completely absent within the tailings layer due to insufficient SO_4. Gibbsite, which dissolved within the waste in Case 1, is here relatively unchanged from its initial volume fraction of 0.005

The pH response is highly dependent on the initial volume fractions of carbonate minerals, which we have assumed here to be limited and uniform for all layers in each cell.

5.3 Discharge Water

Figure 6 shows a direct comparison between the observed and simulated pH and sulphate concentrations in the water discharging from the base of each cell.

In the CCBE-covered cell, the simulated pH of the drainage water remained at near neutral levels of about 6-6.5 for the 1200 day monitoring period. This was in very good agreement with the observed data.

In the non CCBE-covered cell, the simulated pH of the effluent water decreases in several steps which can be correlated to the sequence of pH-buffering minerals mentioned in Section 5.1. Beginning at the initial neutral level of about 6.5 where the pH is buffered by calcite dissolution, the first pH drop in the effluent water occurs at about 150 days, and settles at a plateau of about 5,

buffered by siderite. The next drop occurs at about 300 days, to a pH of about 3.8, buffered by gibbsite. Finally, the pH drops further after about 750 days to about 1.

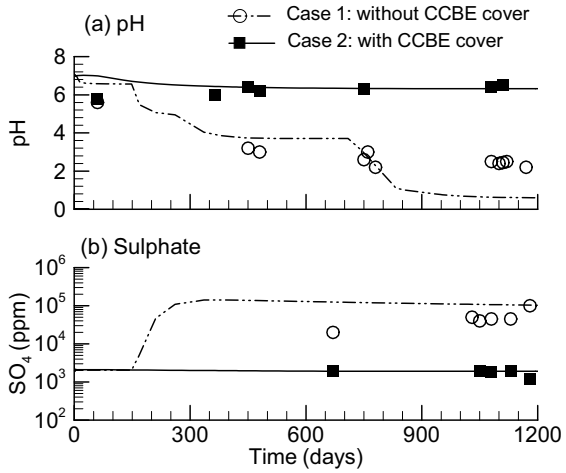

Figure 6. Discharge water evolution over time for the CCBE covered and non-CCBE covered cells. The simulated results (lines) and observed data (symbols) are provided showing the evolution of (a) pH and (b) SO_4 concentrations.

Although the observed pH drop appeared more gradual than the predicted drop, the trends are nevertheless consistent. Gradual pH drops observed in the field and lab at other sites have been attributed to incongruent mineral dissolution (Al et al., 2000), which is not considered in the MIN3P model.

The difference between the simulated effluent pH after 1200 days (pH~1) compared to that observed (pH~2-3) may be due to dilution in the 3D field cell not accounted for in the 1D model. Differences between the observed and simulated behaviour may also be due to a lack of a definitive mineralogical analysis.

The simulated SO_4 concentrations in both cells were also consistent with the observed data (Figure 6). In the CCBE-covered case, the SO_4 concentrations remained near 2000 ppm over the 1200 day period. In the sand-covered cell, however, the predicted SO_4 concentrations began to rise after about 150 days, and increased by about two orders of magnitude (to 10^5 ppm) by 1200 days.

6. CONCLUSIONS

The numerical simulations presented here have helped to show the effect of capillary barrier covers on reducing oxygen diffusion and pyrite oxidation within potentially acid-generating mine wastes. The model is a very useful tool to quantify the coupled effects of groundwater flow and moisture retention on the reactive geochemistry responsible for acid mine drainage.

In these preliminary simulations, discharge from the capillary barrier covered cell was maintained at near-neutral pH, consistent with that observed. Without a capillary barrier cover, the pH in the effluent dropped to about 1 within the tailings effluent. Dissolved iron, sulphate and aluminium concentrations were also significantly reduced in the CCBE cover scenario.

The primary limitations of the model include the neglect of seasonal variations in temperature and recharge, and the uncertainty in the background mineralogy. Carbonate mineralogy, for example, plays a major role in AMD evolution, particularly with respect to pH buffering reactions. More accurate reproduction of field trends will require more thorough and quantitative mineralogical analyses.

7. ACKNOWLEDGEMENTS

We thank Dr. Uli Mayer of UBC for generously supplying the MIN3P code and for his helpful advice. We also thank Lucette Degagné for translating the abstract. Funding for this research was provided in part by the Natural Sciences and Engineering Research Council of Canada through the Polytechnique-UQAT Industrial Research Chair in Environment and Mine Waste Management. The Chair is supported by various industrial and government partners who are listed on the Chair website: http://www.enviro-geremi.polymtl.ca/.

8. REFERENCES

Aachib, M., Aubertin, M., and Mbonimpa, M., 2002. Laboratory measurements and predictive equations for gas diffusion coefficient of unsaturated soils. Proceedings of the 55th Canadian Geotechnical and Joint IAH-CNC and CGS Groundwater Speciality Conferences, Niagara Falls, October 2002, pp. 163-171.

Al, T. A., Martin, C.J. and Blowes, D.W., 2000. Carbonate-mineral/water interaction in sulfide rich mine tailings, Geochim. Cosmochim. Acta 64, pp. 3933-3948.

Aubertin, M., Bussière, B., Monzon, M., Joanes, A.-M., Gagnon, D., Barbera, J.-M., Aachib, M., Bédard, C. and Chapuis, R., 1999. Etude sur les Barrière Sèches Construites a partir de Résidues Miniers : Phase II Essais en Place, NEDEM/MEND Report 2.22.2c.

Bain, J., Blowes, D.W., Robertson, W.D., and Frind, E.O., 2000. Modelling of sulfide oxidation with reactive transport at a mine drainage site. Jour. Contam. Hydrol. 41(1-2), pp. 23-47.

Blowes, D.W., and Ptacek, C.J., 1994. Acid neutralization mechanisms in inactive mine tailings, In: The Environmental Geochemistry of Sulfide Mine-Wastes, Short Course Handbook 22 (eds. D.W. Blowes and J.L. Jambor), Mineralogical Association of Canada, Waterloo, Ontario, pp. 271-292.

Bussière, B., 1999. Etude du comportement hydrique de couvertures avec effets de barrière capillaire inclinées a

l'aide de modélisations physiques et numériques, Ph.D. Thèse, Université de Montréal.

Bussière, B. and Aubertin, M. 1999. Clean tailings as cover material for preventing acid mine drainage: an in situ experiment. Sudbury '99, Mining and the Environment, 1: pp. 19:28.

Bussière, B., Aubertin, M. and Chapuis, R., 2001. Unsaturated flow in layered cover systems : a comparison between numerical and field results. 54th Canadian Geotechnical Conference, Calgary, 3: pp. 1612-161.

Bussière, B., Aubertin, M., and Chapuis, R., 2003. The behaviour of inclined covers used as oxygen barriers. Canadian Geotechnical Journal, 40(3), pp. 512-535.

Davis, G.B., and Ritchie, A.I.M., 1986. A model of oxidation in pyritic mine waste. Part 1: equations and approximate solution. Appl. Math. Model. 10, pp. 314-322.

Jambor, J.L., 1994. Mineralogy of sulfide-rich tailings and their oxidation products, Chapter 3: Short Course Handbook on Environmental Geochemistry of Sulfide Mine Wastes (J.L. Jambor & D.W. Blowes Eds.), Mineralogical Association of Canada.

Joanes, A.-M., 1999. Une analyse hydrogéologique de l'efficacité de recouvrement multicouches pour le drainage minier acide, Mémoire de Maitrise, Génie Civil, Ecole Polytechnique de Montréal.

Johnson, R.H., Blowes, D.W., Robertson W.D. and Jambor J.L., 2000. The hydrogeochemistry of the Nickel Rim mine tailings impoundment, Sudbury, Ontario, J. Contam., Hydrol., 41, pp. 49-80.

Jurjovec, J., Ptacek, C., and Blowes, D., 2002. Acid neutralization mechanisms and metal release in mine tailings: A laboratory column experiment. Geochimica et Cosmochimica Acta 66(9), pp. 1511-1523.

Lefebvre, R., Hockley, D., Smolensky, J., and Gélinas, P., 2001. Multiphase transfer processes in waste rock piles producing acid mine drainage. 1. Conceptual model and system characterization, J. Contam. Hydrol. 52, pp. 137-164.

Mayer, K.U., Frind, E.O., and Blowes, D.W., 2002. Multicomponent reactive transport modeling in variably saturated porous media using a generalized formulation for kinetically controlled reactions. Water Resour. Res. 38(9), 13: pp. 1-21.

Mayer, K.U., Frind, E.O. and Blowes, D.W., 2003. Advances in reactive-transport modeling of contaminant release and attenuation from mine-waste deposits, Chapter 14: Environmental Aspects of Mine Wastes, (J.L. Jambor, D.W. Blowes and A.I.M. Ritchie, Eds.), Short Course Volume 31, Mineralogical Association of Canada, pp. 283-302.

Mbonimpa, M., Aubertin, M., Aachib, M., and Bussière, B. 2003. Diffusion and consumption of oxygen in unsaturated cover materials, Can. Geotech. J., 40, pp. 916-932.

Millington, R.J., and Quirk, J.M., 1961. Permeability of porous solids. Trans. Faraday Soc. 57: pp. 1200-1207.

Molson, J.W., Fala, O., Aubertin, M. and Bussière, B., 2004. Numerical Simulations of Sulphide Oxidation, Geochemical Speciation and Acid Mine Drainage in Unsaturated Waste Rock Piles, in submission to: Environmental Geology.

Nicholson, R.V., Gillham, R.W., Cherry, J.A. and Reardon, E.J. 1989. Reduction of acid generation in mine tailings through the use of moisture-retaining cover layers as oxygen barriers. Canadian Geotechnical Journal, 26: pp. 1-8.

Oldenburg, C., and Pruess, K., 1993. On numerical modeling of capillary barriers. Water Resour. Res. 29(4), pp. 1045-1056.

Pruess, K., 1991. TOUGH2- A general purpose numerical simulator for multiphase fluid and heat transfer. Lawrence Berkeley Laboratory LBL-29400, 102pp..

Romano, C. G., Mayer, K.U., Jones, D.R., Ellerbroek, D.A., and Blowes, D.W., 2003. Effectiveness of various cover scenarios on the rate of sulphide oxidation of mine tailings. Jour. of Hydrology 271, pp. 171-187.

Schneider, P., Osenbrueck, K., Neitzel, P.L., and Nindel, K., 2002. In-situ mitigation of effluents from acid waste rock dumps using reactive surface barriers – a feasibility study. Mine Water and the Environment, 21: pp. 36-44.

Sracek, O., Choquette, M., Gelinas, P., Lefebvre, R., and Nicholson, R.V., 2003. Geochemical characterization of acid mine drainage from a waste rock pile, Mine Doyon, Quebec, Canada. Jour. Cont. Hydrol. 69, pp. 45-71.

van Genuchten, M. Th., 1980. A closed-form equation for predicting the hydraulic conductivity of unsaturated soils. Soil Science Society of America Journal, 44: pp. 892-898.

Wösten, J.H.M., and van Genuchten, M.Th., 1988. Using texture and other soil properties to predict the unsaturated soil hydraulic functions, Soil Sci. Soc. Am., J., 52, pp. 1762-1770.

Wunderly, M.D., Blowes, D.W., Frind, E.O., and Ptacek, C.J., 1996. Sulfide mineral oxidation and subsequent reactive transport of oxidation products in mine tailings impoundments: A numerical model. Water Resour. Res. 32(10), pp. 3173-3187.